N O T I C E

THIS DOCUMENT HAS BEEN REPRODUCED FROM MICROFICHE. ALTHOUGH IT IS RECOGNIZED THAT CERTAIN PORTIONS ARE ILLEGIBLE, IT IS BEING RELEASED IN THE INTEREST OF MAKING AVAILABLE AS MUCH INFORMATION AS POSSIBLE

NASA

Technical Memorandum 82023

A Description of the NSSL Cases Used for a Simulated VAS Retrieval Study

Anthony Mostek, Louis Uccellini and Wally Gross

OCTOBER 1980

NASA

Technical Memorandum 82023

A Description of the NSSL Cases Used for a Simulated VAS Retrieval Study

Anthony Mostek, Louis Uccellini
and Wally Gross

OCTOBER 1980

A DESCRIPTION OF THE NSSL CASES USED FOR A

SIMULATED VAS RETRIEVAL STUDY

Anthony Mostek
Computer Sciences Corporation
System Sciences Division
8728 Colesville Road
Silver Spring, Maryland

Louis Uccellini
Code 914
Goddard Laboratory for Atmospheric Sciences
Goddard Space Flight Center
Greenbelt, Maryland

and

Wally Gross
Computer Sciences Corporation
System Sciences Division
8728 Colesville Road
Silver Spring, Maryland

October 1980

TABLE OF CONTENTS

LIST OF TABLES

LIST OF ILLUSTRATIONS

v

Page intentionally left blank

A DESCRIPTION OF THE NSSL CASES USED FOR A SIMULATED VAS RETRIEVAL STUDY

Anthony Mostek[*]
Louis Uccellini[†]
and
Wally Gross[*]

ABSTRACT

A documentation of eight NSSL severe storm cases, which serve as a basis for a simulated VAS retrieval study is presented in this paper. Six of the selected cases provide a control data set to be used to complete the statistical information needed for retrieval techniques based upon the use of regression matrices. The other two cases (May 22 and May 29, 1976) are to be used in the actual retrieval experiments (Chesters, et al., 1980). The selection is based upon the presence of moisture gradients in the analysis region, the availability of satellite images at the selected time periods, and the extent of cloud cover within the observing network.

---

[*]Computer Sciences Corporation, System Sciences Division, 8728 Colesville Road, Silver Spring, Maryland

[†]Code 914, Goddard Laboratory for Atmospheric Sciences, Goddard Space Flight Center, Greenbelt, Maryland

A DESCRIPTION OF THE NSSL CASES USED FOR A SIMULATED VAS RETRIEVAL STUDY

1. INTRODUCTION

A major research effort outlined in the Project Plan for the VISSR Atmospheric Sounder (VAS) Demonstration is a sounding simulation experiment designed to (1) implement software that simulates VAS radiances for severe storm environments (Chesters and Carter, 1980), (2) estimate the extent to which the VAS radiance information depicts temperature and moisture gradients in a severe storm environment (Chesters *et al.*, 1980), and (3) determine the relative sensitivity of a regression and least-squares retrieval technique (Lee and Chesters, 1980) to statistical conditioning.

The retrieval schemes implemented on the GSFC VAS Processor are conditioned by historical data to yield retrieved temperature and moisture profiles within a mesoscale environment. The mathematical inverse of a noisy radiation transfer process is not uniquely determined. It is, there-fore, necessary to constrain the solution to be consistent with the meteorological information gleaned from independent observing systems or from historical data sets. In particular, the statistical nature of meteorological sounding sets can be incorporated directly into the retrieval technique through the derivations of linear regression matrices based upon soundings that are representative of specific meteorological events like severe storms and tropical storms. Therefore, the experiment is designed to determine if ancillary data that is representative of the severe storm environment can be incorporated within the retrieval scheme to yield more accurate soundings.

1

The purpose of this Technical Memorandum is to document eight severe storm cases that are to be applied in the simulation study (Chesters, *et al.*, 1980). The storms all occurred in the 1976 National Severe Storm Laboratory (NSSL) mesoscale network and represent a reasonable cross-section of various synoptic conditions that lead to severe weather in the Great Plains. The data from the NSSL provide a mesoscale perspective of the severe weather outbreaks, which makes them compatible for VAS sounding experiments, given the projected 30-to-90 km resolution of the VAS. The methodology for generating the data sets is described in Section 2. A brief description of the six cases used to generate the climatological statistics is presented in Section 3. In Section 4, a more detailed description of the two cases used in the actual simulation experiments is provided.

2. DATA SET GENERATION USING A BARNES OBJECTIVE ANALYSIS

In order to utilize the NSSL observations, the irregularly spaced data must be interpolated to a three-dimensional grid (Barnes, *et al.*, 1971). The Barnes objective analysis scheme, which allows for data drifting with respect to time (see Barnes, 1973), is used to generate the three dimensional grids needed for the sounding simulation study. Values of temperature, dewpoints and winds are determined at regularly spaced grid points through the application of a weighted average of the neighboring observations. The weighting varies with respect to the distance of the measured values to the grid point. Barnes' process applies both a space and time mean to the derivations. Once the grid has been established, it is rotated so that the x-axis will be aligned parallel to the motion of the storm system. The data are also drifted in time in the x-direction with the speed of the system, a procedure that enables the observations to maintain their same relative position to the storms. Thus, the computed field (ϕ_{ij}) at a given grid point (X_i, X_j) is given by

$$\phi_{ij} = \frac{\Sigma \, \phi_k \, w_k \, w_k'}{\Sigma \, w_k \, w_k'} \qquad (1)$$

2

where ϕ_k is the kth observation and

$$w_k = \exp - \left[\frac{(X_i - X_k)^2 + (Y_j - Y_k)^2}{\sigma_D} \right] , \qquad (2)$$

is the distance-weighting factor,

$$w_k' = \exp - \left[\frac{(t_{map} - t_k)^2}{\sigma_t} \right] . \qquad (3)$$

is the time-weighting factor; (t_k, X_k, Y_k) are the time and position of the kth observation; σ_D and σ_T are the space and time weighting factors; and t_{map} is the analysis time.

The root mean square (RMS), which gives a measure of the error in the computations, is determined by calculating the differences between the observations and the interpolated values at these points, so that

$$RMS = \left(\frac{\Sigma w_k \epsilon_k^2}{\Sigma w_k} \right)^{\frac{1}{2}} , \qquad (4)$$

where ϵ_k is the error between the kth observation and the analyzed field interpolated to the point of that measurement. If the RMS is too large, a correction is applied by interpolating the differences between the analyzed field and the observations to the analysis grid and performing another interation. This process typically has a practical limit of three or four adjustments, after which the error reduction is negligible.

The following six parameters must be defined to perform the analysis: the speed and direction of the storm complex, the size and location of the analysis grid, the time and space weighting factors σ_T and σ_D. The speed and directions of the storms are determined subjectively from measurements of Oklahoma City WSR-57 radar pictures compatible with the NSSL observations. The network is encompassed in an 11-by-21 grid with 20-km spacing, centered at 10.6 km south of

3

Hinton, Oklahoma (35.4°N and 98.4°W), a domain which includes all nine NSSL stations (Figure 1). σ_D and σ_T are determined subjectively by reducing the RMS error of the output fields. Since the NSSL data are divided into 90-minute time steps and the stations are separated by approximately 60 to 70 kilometers, a reasonable first guess for the two variables would be $\sigma_D = 3600$ (60^2) and $\sigma_T = 8100$ (90^2). A smaller value of σ_D will provide detailed representations of the field in an area of high data density, yet difficulties will be encountered in data sparse regions (Figure 1). These problems are most readily adjusted for by selecting a medium range for σ_D. If the value is too large, the resultant field will be smoothed to such a nonrepresentative degree that the RMS will become excessively large.

The historical and future configurations of the data can be included in the determination of the field, as long as a proper value is assigned to σ_T. Since the data are drifted along with the storm
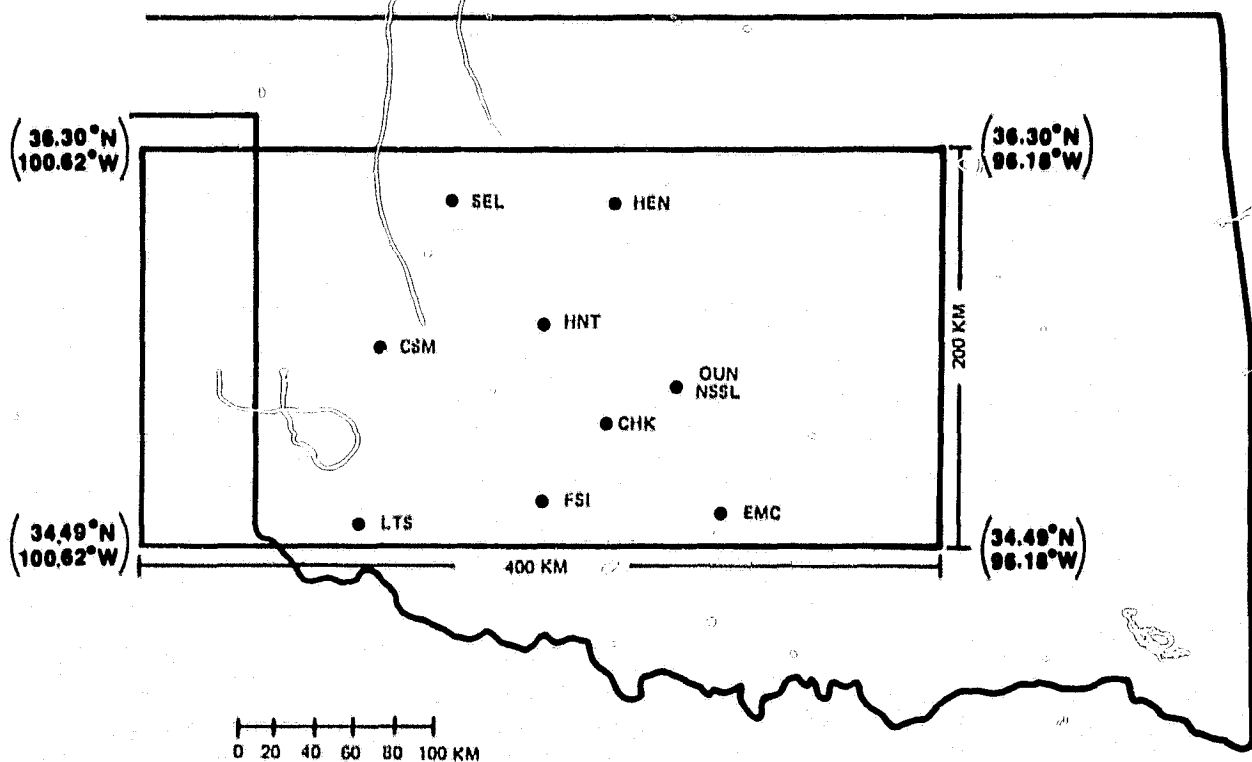

Figure 1. Analysis region showing the location of the nine 1976 NSSL stations.

systems, the overall configuration of the meteorological parameters with respect to the storms will be maintained. An exponential weight is applied which causes a rapid decrease in the importance of the surrounding time periods, especially by the third time step. Thus, a rather large value of σ_T (18,225) is applied and a centrally time-weighted condition is maintained. These selected values of σ_D and σ_T are not final and can be varied to meet the specifications of any given situation. On a final note, the actual calculations were conducted using a Mercator projection true at a latitude (35.4°N) through the center of the special domain. This adjustment facilitated the derivations, while only introducing a slight error at the boundaries on the order of 0.01 degree. Therefore, some minor errors will be encountered when the data fields are navigated onto a satellite image during the cloud-correction phase of the simulation experiment.

3. BRIEF DESCRIPTION OF THE SIX NSSL CASES USED TO DERIVE CONDITIONED REGRESSION MATRICES

Eight NSSL cases were selected from the Spring 1976 field experiment which collected data on 17 dates. Six of these dates were chosen to provide a data base for statistical purposes, while the other two dates were selected as target cases for the full VAS retrieval demonstration. The six conditioning cases were chosen for the study after our review of the synoptic maps revealed that these dates are fairly representative of environmental conditions suitable for the development of severe convective storms. These conditions ranged from cyclones and their associated frontal systems to the formation and propagation of drylines through the special network. A listing of the six NSSL cases is provided in Table 1 and summarized below.

a. May 12, 1976 (NSSL Number 28)

A low pressure system moved across the NSSL network from the Texas Panhandle with an attending cold front sweeping through the region. Ample upper air support was available for severe storm development as a trough amplified over the northern Rockies and propagated towards the

5

Table 1. 1976 NSSL Data Sets

Date	Number of Soundings	NSSL Case Number	Time Span of Soundings (GMT)	Description of Storm Activity
May 12, 1976	35	28	1500 to 2200	A strong squall line oriented from east-to-west moving to the south through the network associated with cyclogenesis in Texas panhandle.
May 21, 1976 through May 22, 1976	44	37	1500 to 0100	Scattered storm cells near the northwest corner of the network associated with a stalled leeside trough to the west of the Oklahoma area.
May 26, 1976	35	42	1500 to 2200	Areas of scattered activity developed over the network near the warm and cold fronts associated with a low pressure system that moved over the area from the Texas panhandle.
June 12, 1976	45	59	1500 to 2330	Few cells near northwestern corner of observation ahead of dryline slowly propagating east toward the network.
June 14, 1976 through June 15, 1976	65	61	2200 to 0300	Strong storm developed in response to significant short wave propagating southeast over network and initiated by the intersection of frontal boundary with pre-existing dryline.
June 17, 1976 through June 18, 1976	44	62	2300 to 0530	Strong storms developed in response to frontal and dryline interaction as weak short wave propagated eastward through network.

western Plains. At 1900 GMT, sharp gradients in the moisture and temperature fields existed over the NSSL network as the cooler and drier air behind the front advanced into the hot, moist air that dominated the eastern half of Oklahoma. By 2200 GMT, the sharp gradients in the temperature field had moved off to the east as a smooth, cooler field now presided over the network. A sharp discontinuity remained in the moisture field, while the drier air slowly moved in over the western half of the area.

b.   May 21, 1976 (NSSL Number 37)

A blocking ridge in the upper level flow over the Gulf coast was beginning to break down, which allowed a divergent flow pattern to move in towards the network. On the surface, a stalled front associated with a leeside trough was starting to show signs of movement with the alteration in the upper level flow. The temperature field indicated warmer air in the northern sections while the moisture field was homogeneously wet over the entire domain. The blocking pattern remained strong enough to prevent the drier and cooler air from moving across into the network, and the storm activity rapidly decayed as it outran its support when reaching Oklahoma.

c.   May 26, 1976 (NSSL Number 42)

A surface low over the Texas panhandle with a warm front extending eastward through Oklahoma and a cold front pushing east towards the network provided classic storm conditions on this date. The mesoscale temperature analysis at 2030 and 2200 GMT depicts pockets of warm air moving to the east across the southern half of the domain, which provided sharp temperature gradients. The dewpoint analysis revealed some drier air associated with the warmer temperatures, which established some weak variations in the moisture field.

d. June 12, 1976 (NSSL Number 59)

Another blocking ridge over the Gulf coast in the upper level flow produced an almost stagnant situation over the network. However, a surface dryline was located across the network, which is readily apparent from an 850-mb mesoscale analysis at 2030 GMT. The temperature field at this time was actually warmer to the north in the drier airmass, which provided a northwest to southeast gradient over the special grid. Only slight changes occurred in the fields from 2030 to 2330 GMT, which resulted in scattered storm activity across the northwestern corner of the network.

e. June 14, 1976 (NSSL Number 61)

An upper level trough moving down from Idaho over Wyoming provided the support for a surface cold front to advance towards the special domain. A cooler air mass over the eastern regions of the grid at 2200 GMT was gradually replaced by warmer air advecting from the west. Cooler air then pushed down from the north in association with the front, which maintained a significant temperature gradient over the area. The 850-mb dewpoint temperature field maintained a pattern of drier air to the north, which coincided with the gradual frontal motion for this case.

f. June 17, 1976 (NSSL Number 62)

Strong upper air support in the form of a long wave trough moving across from the Rocky mountains towards the plains helped force a cold front from Colorado into southeastern Oklahoma. The temperature field at 850 mb began to show the intrusion of cooler air into the western region of the special grid by 2330 GMT. A sharp temperature gradient moved across the network towards the east as the cooler air continued flowing in from the west over the next 6 hours. The dewpoint temperatures at the same level showed drier air moving rapidly across to the east behind the front. The sharp gradients present in temperature and moisture fields along the front provided adequate support for the storm activity propagating across the network on this date.

4. A DETAILED ANALYSIS OF TWO NSSL CASES USED FOR THE VAS SIMULATION STUDIES

Two 1976 NSSL cases were selected for the simulated VAS retrieval study since they are representative of the severe storm environment encountered in the southern Great Plains and contain moisture and temperature gradients that should be detectable by the VAS channels. A description of the two cases is given in this section in order to outline the time periods that are optimal for generating the simulated radiances for the retrieval study (Chesters *et al.*, 1980).

a.   May 22, 1976 (NSSL Case Number 38)

This case provides the most extensive data set with 80 soundings having been taken from 1500 GMT on May 22, 1976 to 0530 GMT on May 23, 1976, and contains an example of a squall line developing in the Texas panhandle and rapidly propagating eastward directly over the NSSL network. An in-depth analysis of the kinematic and dynamic aspects of this storm system is presented in the investigation by Ogura and Liou (1980).

The National Weather Service Surface Analysis at 2100 GMT (Figure 2), when the squall line is developing in Texas, depicts a double low pressure system in northcentral Kansas and western Texas with a cold front connecting the two cyclones. A rapidly developing situation is evident in that appreciable pressure falls of two millibars or more are present throughout the region ahead of the low pressure centers. Adding to the evolution of the storm environment is a wedge of dry air beginning to accelerate towards the northeast from southwestern Texas. This dryline is marked by dewpoint temperatures that range from readings in the 60s down into the 30s across this frontal zone. Figure 3 shows the 500-mb chart for 0000 GMT May 23, 1976. The combination of the waves over Louisiana and Colorado produces a difluent flow over the Oklahoma area. At this time, the storm complex is developing rapidly and propagating to the east along the western boundary of the special grid (Figure 1), which would place the squall line near the Texas Panhandle—Oklahoma border.
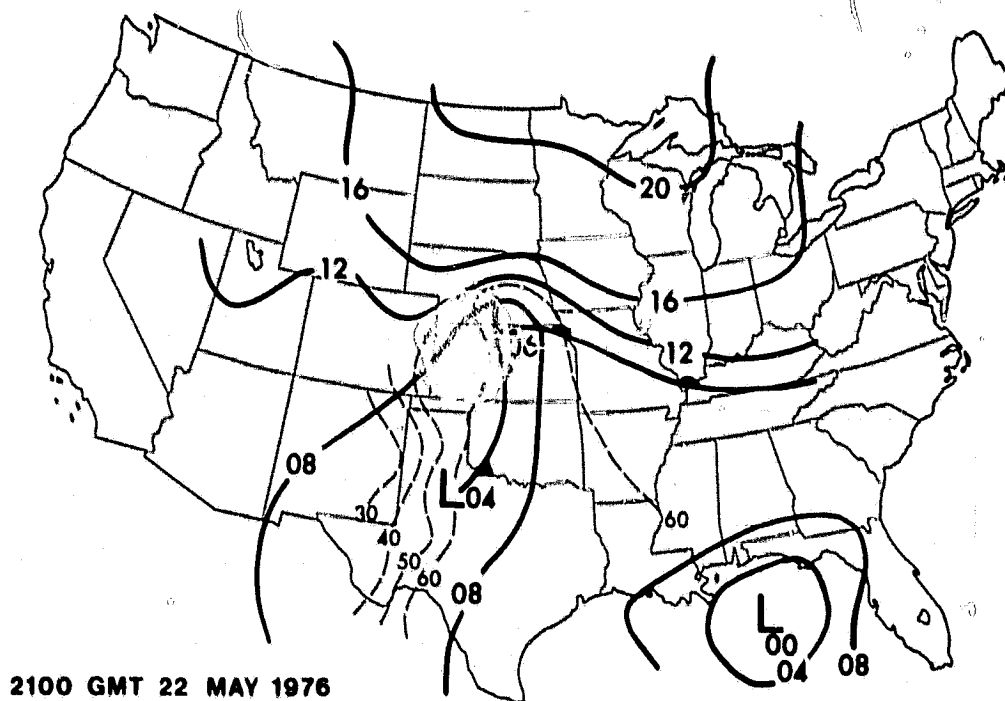
2100 GMT 22 MAY 1976

Figure 2. Surface analysis, pressure (mb) and dewpoint temperature (F), at 2100 GMT 22 May 1976.

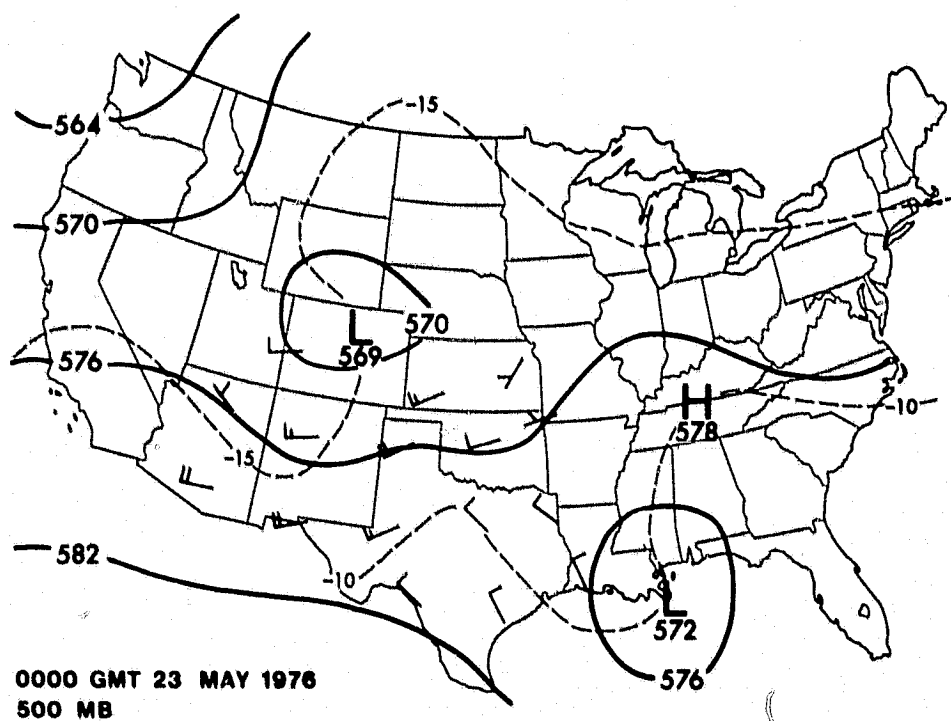**0000 GMT 23 MAY 1976**
500 MB

Figure 3. 500-mb analysis, geopotential (dm, 570 = 5700 gpm), wind barbs (ms^{-1}) at 0000 GMT 23 May 1976.

Another important aspect of the environmental conditions is the variation in cloud cover over the NSSL area. This condition is of prime importance in selecting an appropriate time period for the retrieval, since extensive cloudiness could interfere with the simulation procedure. Figures 4, 5 and 6 provide satellite images for 2330 GMT May 22, 1976 (visible and infrared) and 0100 GMT May 23, 1976 (infrared). The pre-squall line atmosphere is relatively clear over the network at 2330 GMT. By 0100 GMT, the cloud cover associated with the storm system is overspreading much of the western half of the grid area. Some partly cloudy to clear regions are still evident, especially
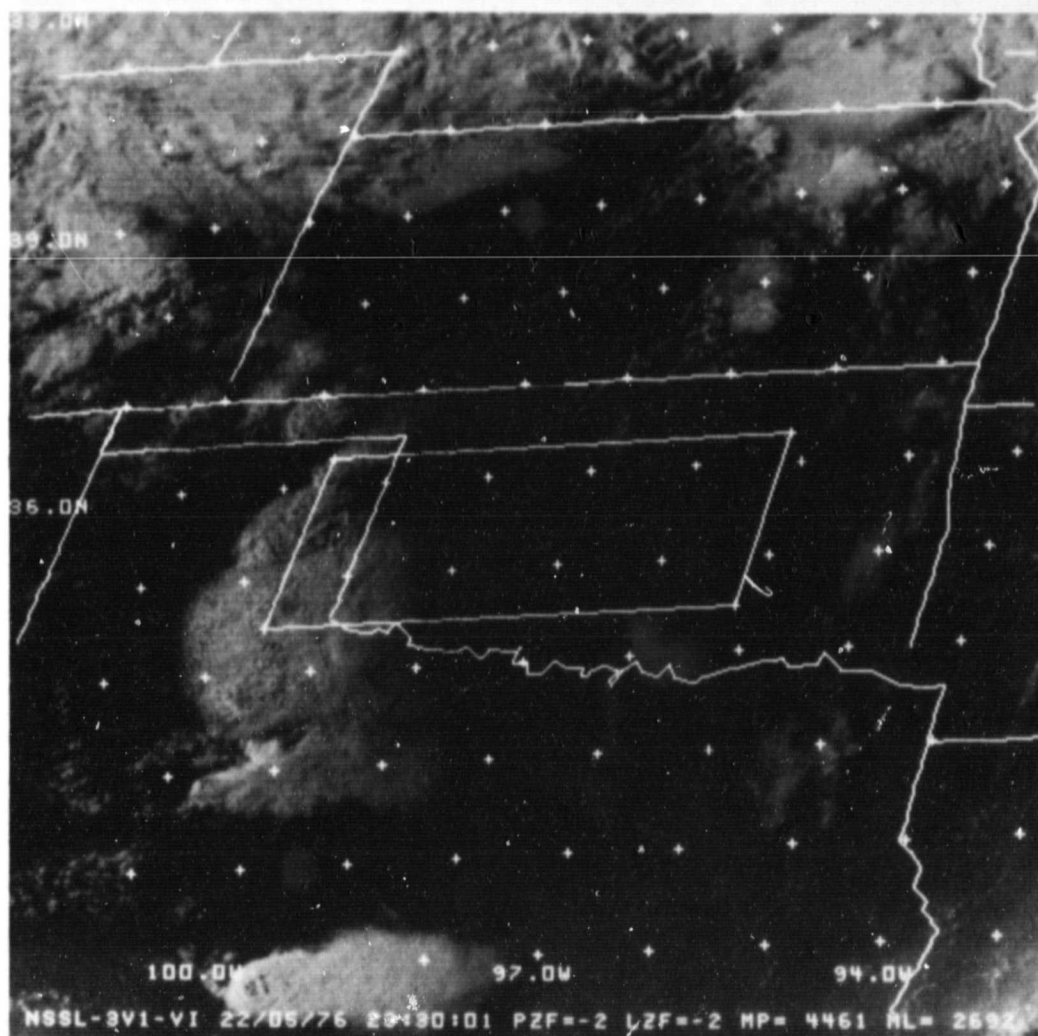

Figure 4. SMS-GOES visible image depicting NSSL analysis region at 2330 GMT 22 May 1976.
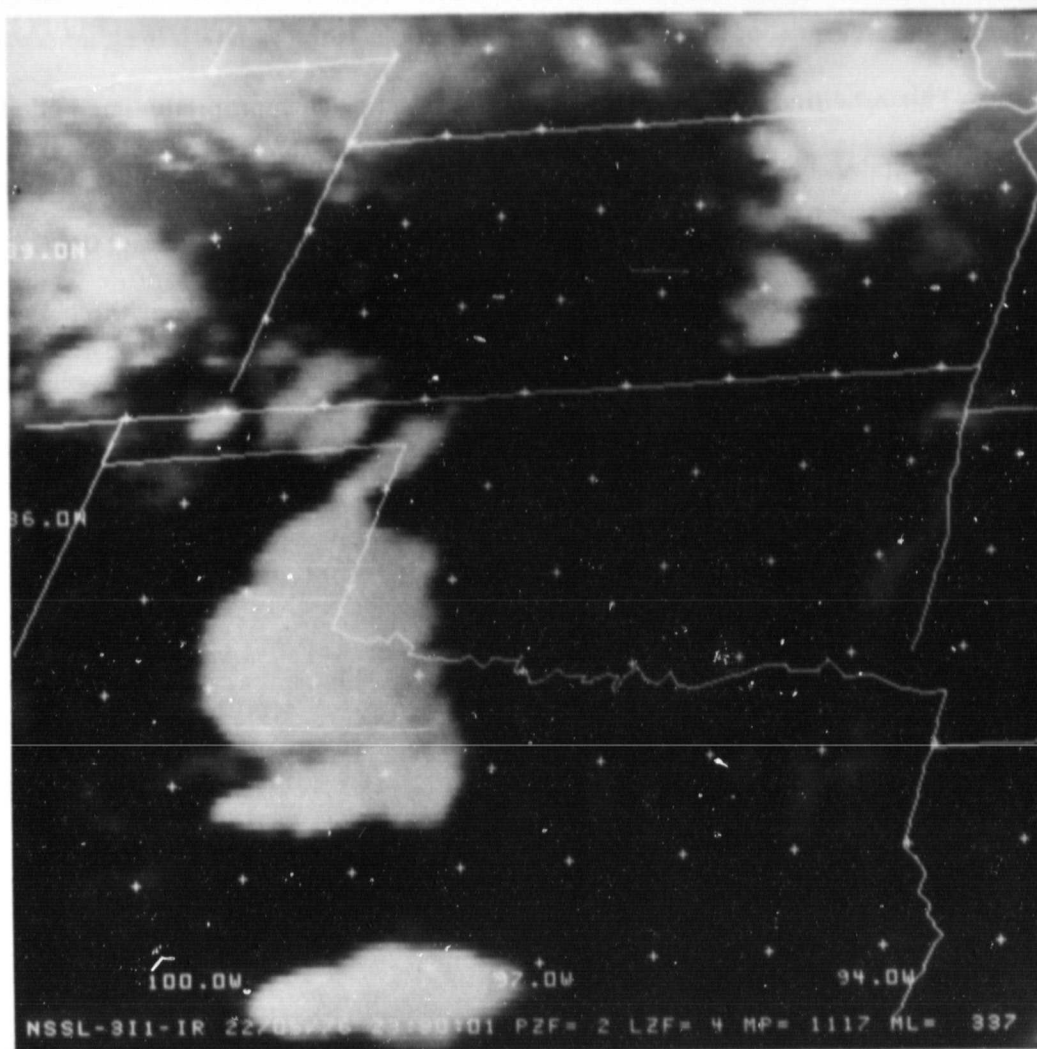
11

Figure 5. SMS–GOES infrared image depicting NSSL analysis region at
2330 GMT 23 May 1976.

over the eastern portions. More extensive cloud cover continued to develop at later times, which

severely restricted the areas that could be incorporated into the retrieval study. These satellite

images will also be included in the procedure that allows for a correction factor to be applied to

broken cloud cover in the generation of simulated VAS radiances (Chesters and Robinson, 1980).

In establishing an optimum time period for the simulation study, the meteorological environ-

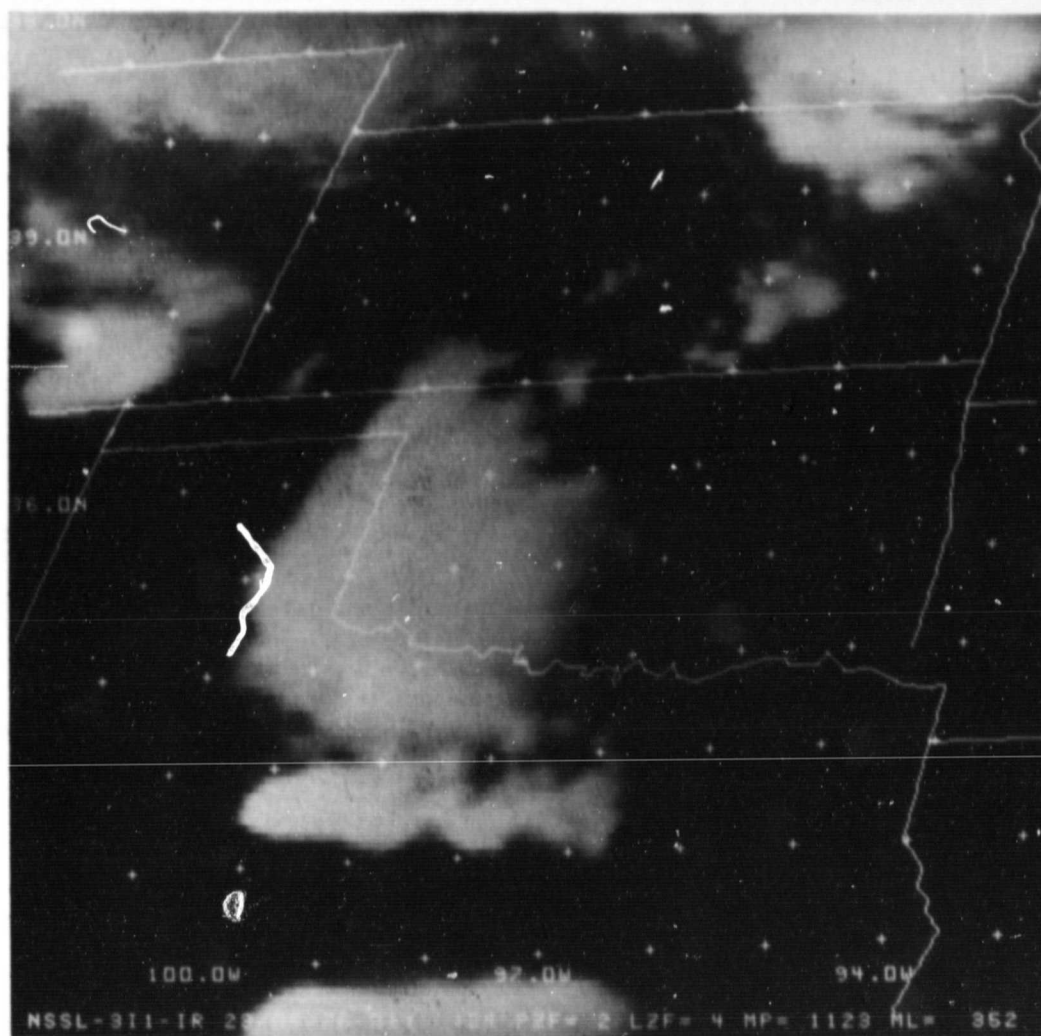ment over the domain must also be examined closely. The weather variables are contained

Figure 6. SMS-GOES infrared image depicting NSSL analysis region at
0100 GMT 23 May 1976.

in various three–dimensional data fields, which were generated as described in Section 2. The 850–

mb temperature fields at 2330 and 0100 GMT May 22–23, 1976 (Figures 7 and 8) describe the

contrast present along the squall line, which is oriented north–to–south. A pocket of cooler air

$(T_{850} = 280°K (15°C))$ advects into the grid from the northwest, probably representing the outflow

of the storm complex. The dewpoint temperatures at 850 mb (Figures 9 and 10) also depict a

sharp temporal variation, especially through the western portions of the network, as the storms pass

across the region.

13

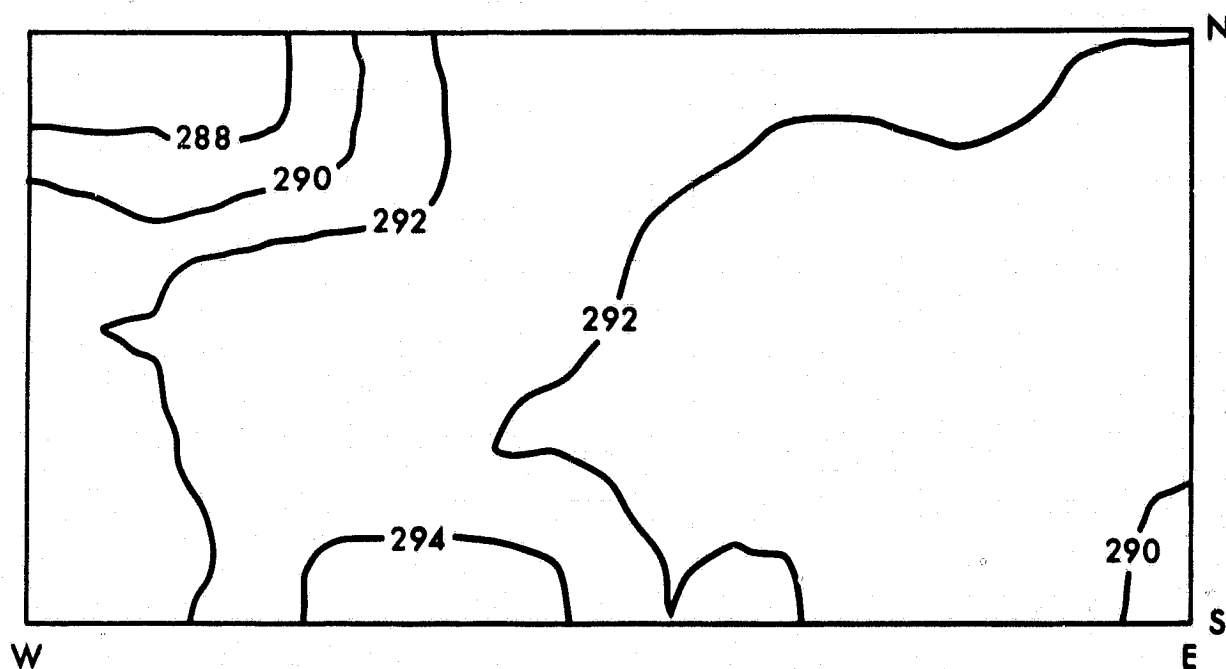Figure 7. 850-mb temperature (K) analysis for special NSSL grid at 2330 GMT 22 May 1976.

Figure 8. 850-mb temperature (K) analysis for special NSSL grid at 0100 GMT 23 May 1976.

Figure 9. 850-mb dewpoint temperature (K) analysis for special NSSL grid at 2330 GMT 22 May 1976.
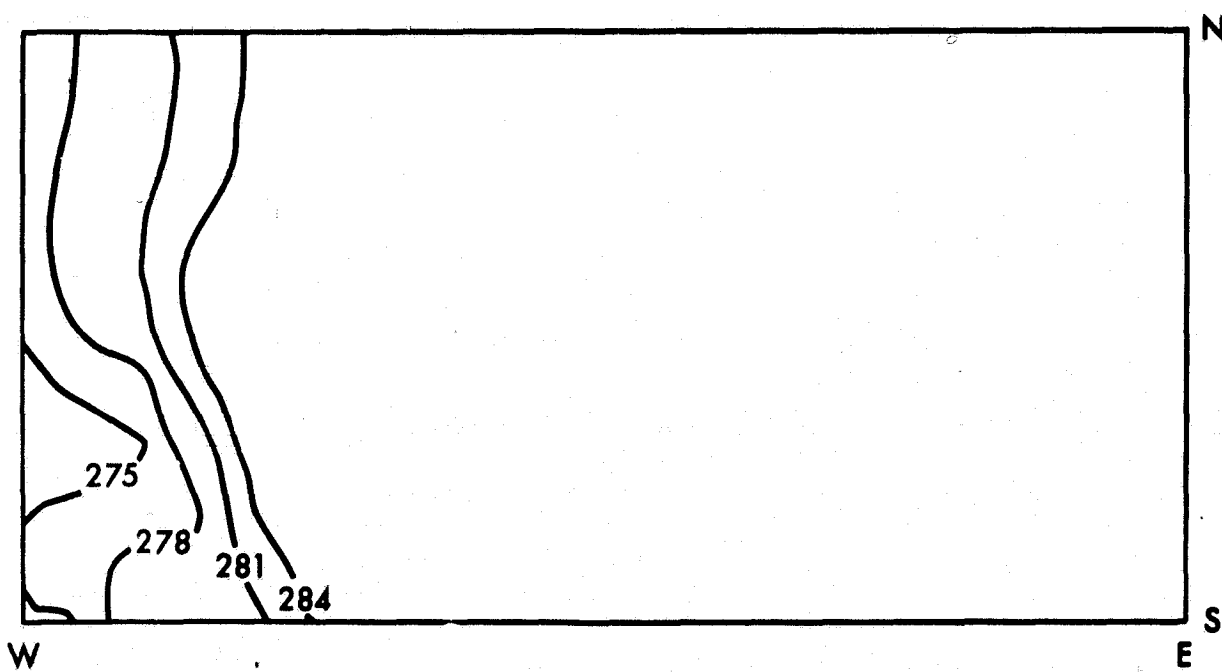

Figure 10. 850-mb dewpoint temperature (K) analysis for special NSSL grid at 0100 GMT 23 May 1976.

A vertical view of the mixing ratio field (Figures 11 and 12), taken along an east-west line through the center of the grid, shows the moist air advecting into the region from the west at 2330 GMT. A bubble shape is seen in the field along the 1.6g/kg contour and with the apparent inflow at the lower levels along 11.4g/kg. By 0100 GMT, the wettest air moved in over the center of the network, while drier air swept in from the west. An interesting feature of this field is apparent from the bulging of the moist air rising from the low levels at the center of the grid up through the mid-troposphere, which tilts towards the west with height. This same feature is apparent in Ogura and Liou's (1980) Figure 20 and is consistent with the dynamics of an updraft/downdraft circulation within the squall line.
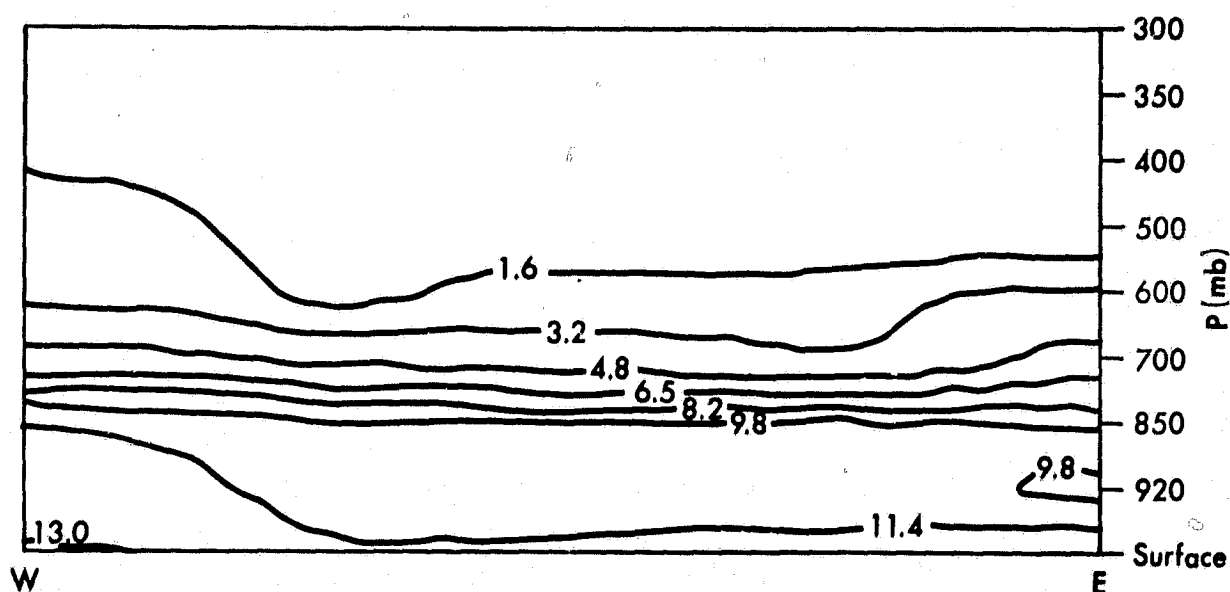

Figure 11. Vertical west-east cross-section of mixing ratio field (g/kg) through the center of the special NSSL grid at 2330 GMT 22 May 1976.
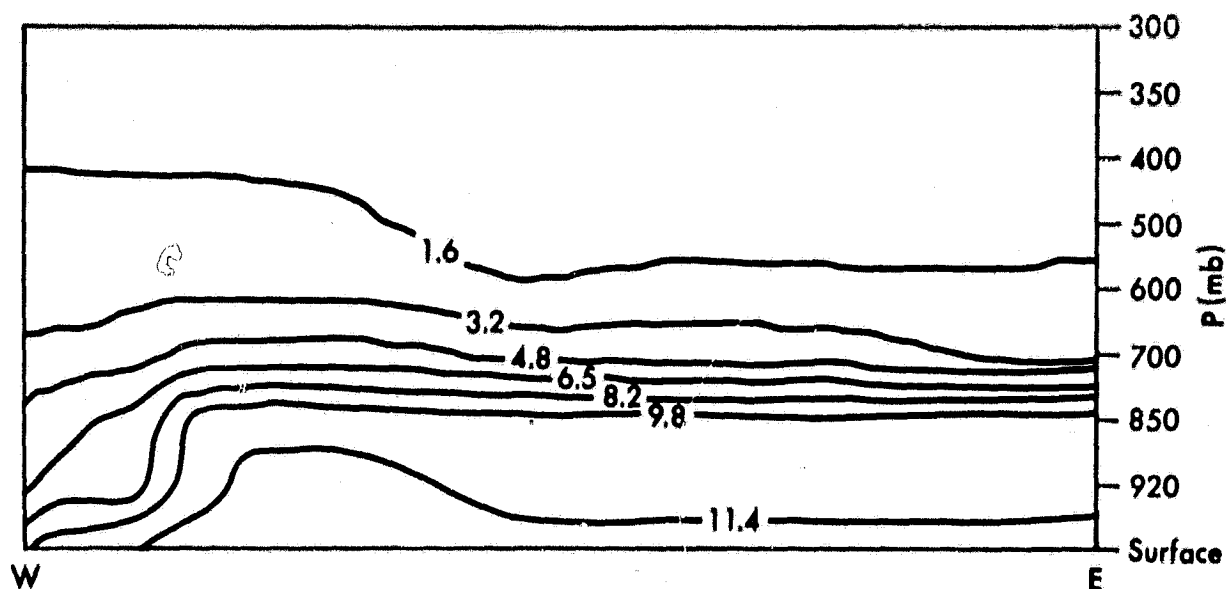
16

Figure 12. Vertical west-east cross-section of mixing ratio field (g/kg) through the center of the special NSSL grid at 0100 GMT 23 May 1976.

The low level equivalent potential temperature (θ_e) field (Figure 13) increased in magnitude through 0100 GMT May 23 ahead of the squall line that moved into the network and indicated that the pre-storm environment was becoming more convectively unstable. After the passage of the squall line at 0230 GMT, the θ_e field became more uniform with θ_e gradually increasing with height, indicating a more stable post-squall line atmosphere.

When this case is actually applied in the simulated VAS retrieval study, the ultimate check of the analysis will be the ability of the simulated radiances to accurately depict the temperature and moisture gradients present over the network as reproduced through the retrievals. A problem area with this case is that the gradients are positioned near the storm system and may be found to be obscured by the cloud cover. Thus, an analysis of the post-storm conditions, which contain the sharpest gradients, may be prevented.
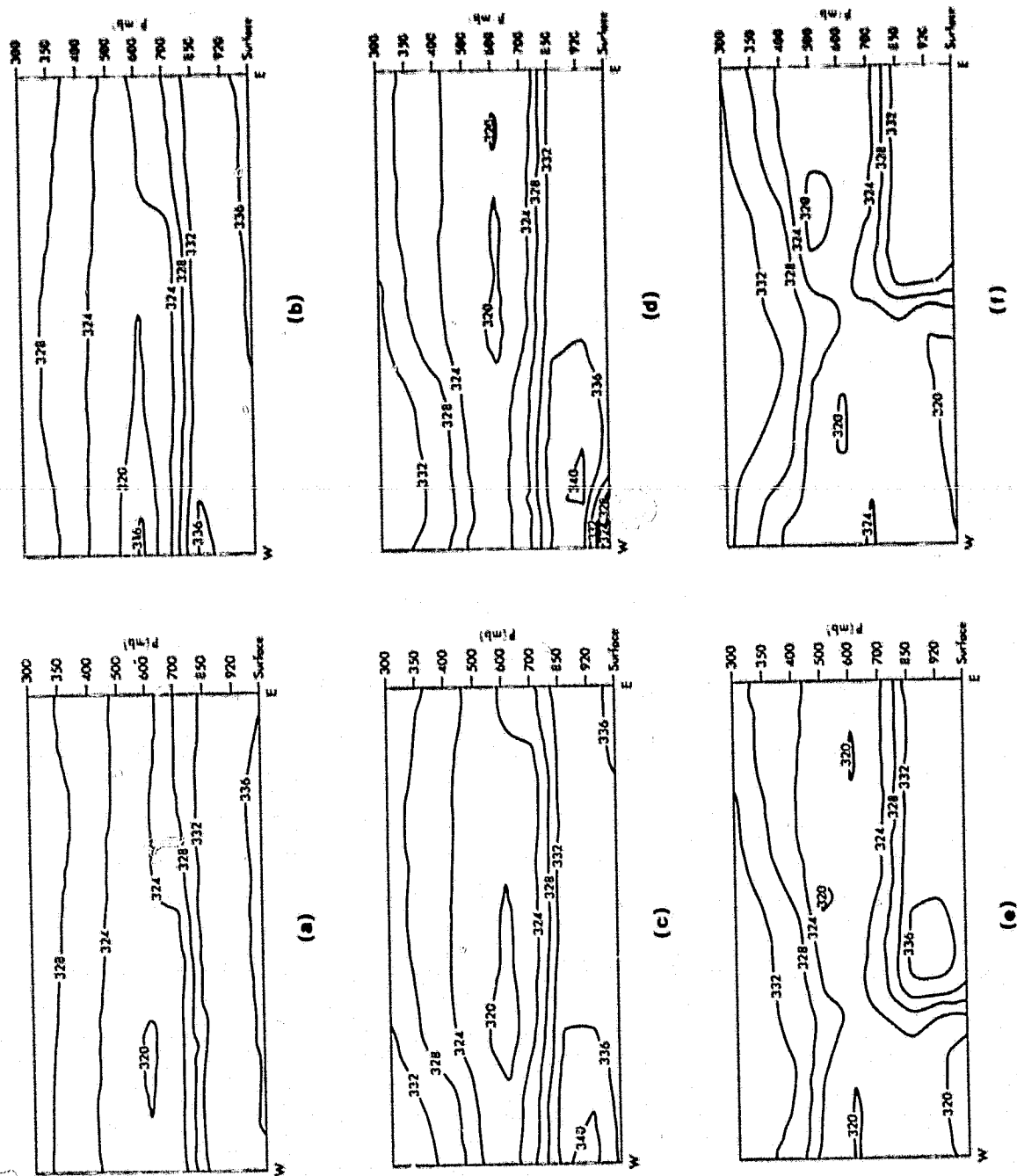
Figure 13. Vertical west–east cross-sections of equivalent potential temperature (K) field through the center of the special NSSL grid at the following times: (a) 2030 GMT 22 May 1976, (b) 2200 GMT, (c) 2330 GMT, (d) 0100 GMT 23 May 1976, (e) 0230 GMT, (f) 0400 GMT.

18

b. May 29, 1976 (NSSL Case Number 45)

The mesoscale data set for this date is not quite as extensive as in the previous case with 55 soundings obtained from 1500 GMT, May 29, 1976 to 0400 GMT May 30, 1976. A supercell storm moved over the NSSL network on this occasion, which produced a downburst as it passed through Oklahoma City, yielding a sudden rise in temperature at the surface.

The National Weather Service Surface Analysis at 0000 GMT May 30, 1976 (Figure 14) shows a moderately strong low pressure system centered over the Texas panhandle. A cold front slices from the low towards the northeast through Oklahoma and into Kansas. Pressure falls ahead of the low were generally over one millibar. A sharp gradient was again present in the dewpoint
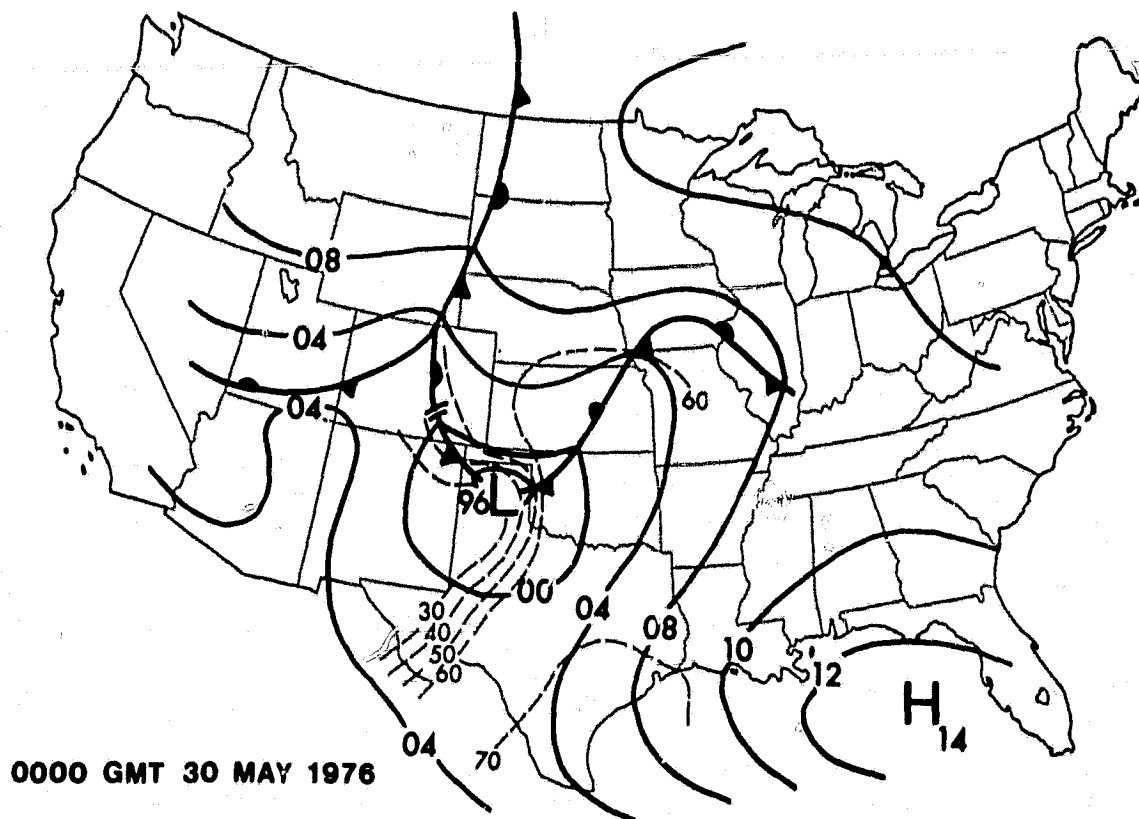

0000 GMT 30 MAY 1976

Figure 14. Surface analysis, pressure (mb) and dewpoint temperature (F) at 0000 GMT 30 May 1976.

19

temperature field with a range from near 20°F in western Texas to 70°F through the middle of the NSSL network. Thus, a rather strong dryline moved across southwestern Oklahoma. Low level convergence associated with the approaching dryline was discernable (from the windfield) across the network region.

The 500-mb chart at 0000 GMT May 30, 1976 (Figure 15) shows generally weak zonal flow over the southwest with just a slight diffluent condition in the Texas–Oklahoma region. A ridge which had been present over the area at the 1200 GMT May 29, 1976 analysis weakened, and this situation aided in the development of the storms observed on this date.

The satellite images in Figures 16 (2030 GMT) and 17 (2330 GMT) show that the supercell was already well over the network grid by the later time. These pictures also provide an indication
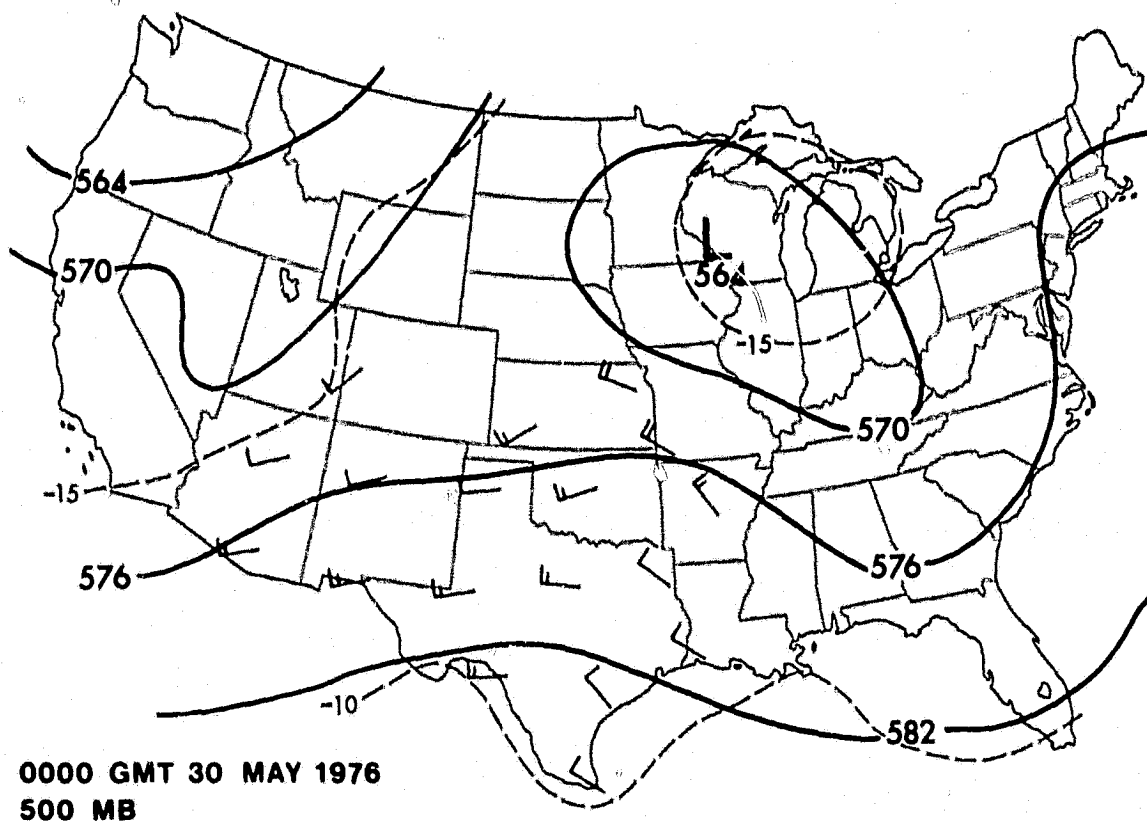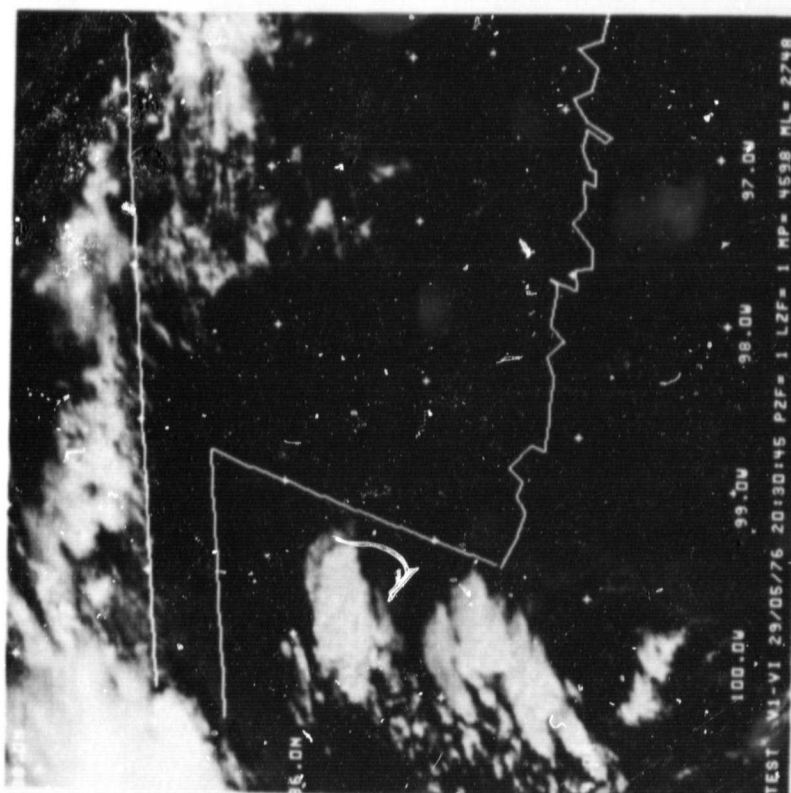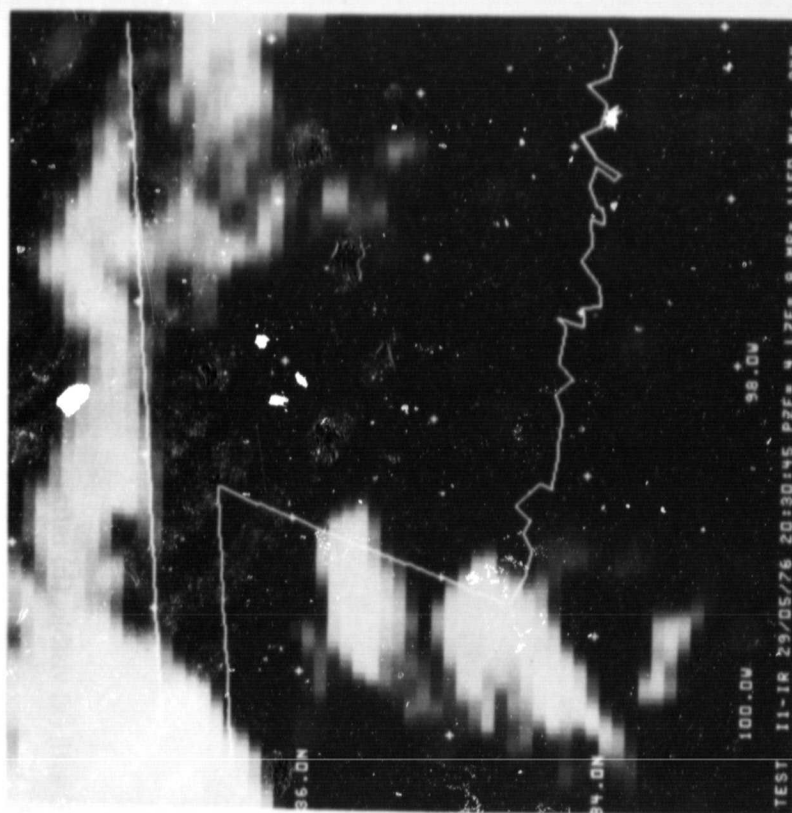

0000 GMT 30 MAY 1976
500 MB

Figure 15. 500-mb analysis, geopotential (dm, 570 = 5700 gpm), wind barbs (ms^{-1}) at
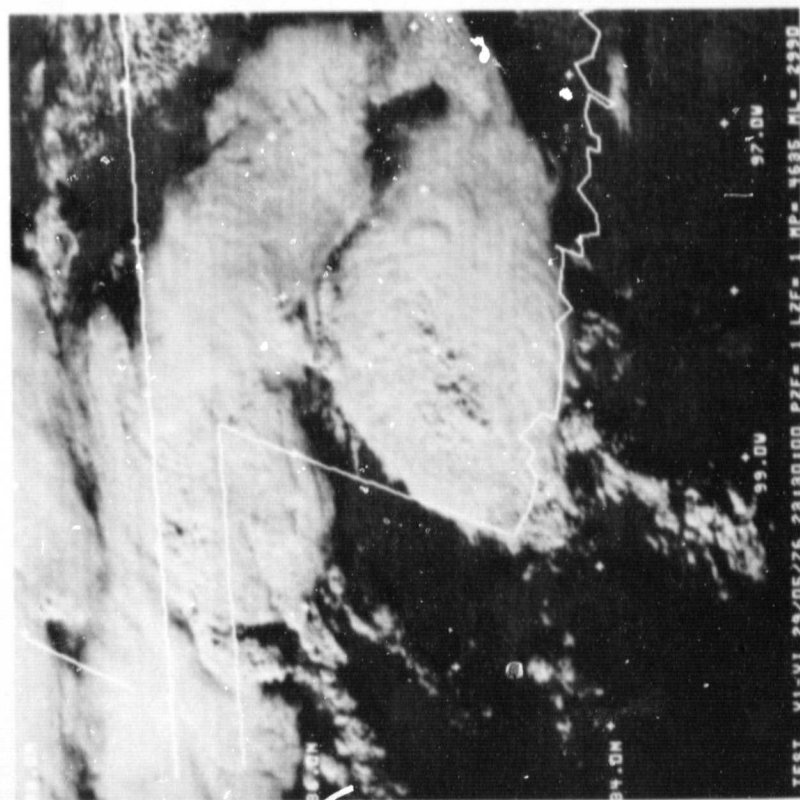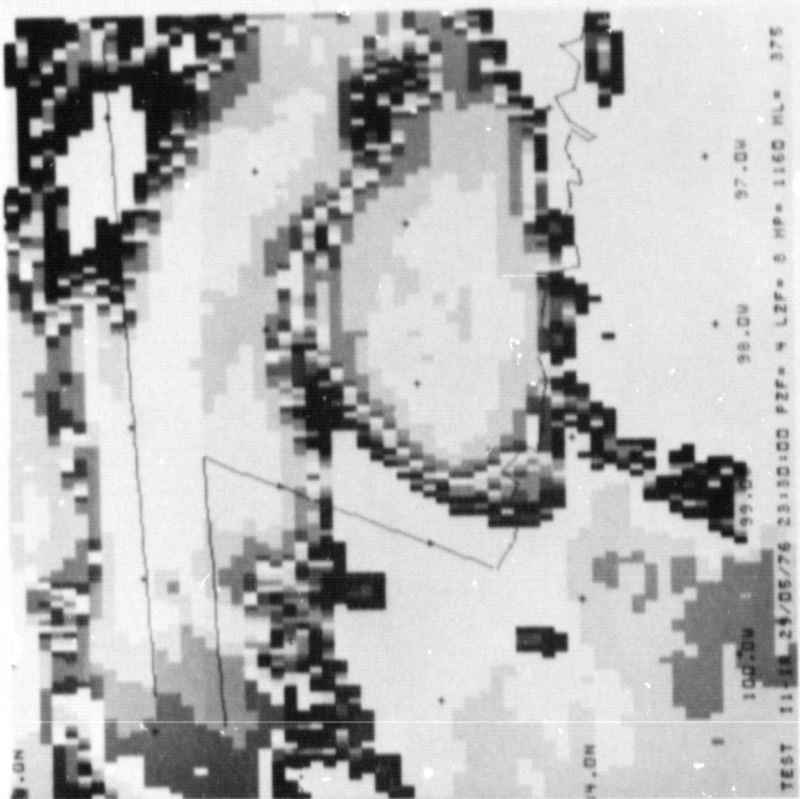0000 GMT 30 May 1976.

20

Figure 16. SMS–GOES images of NSSL analysis area at 2030 GMT 29 May 1976 with (a) visible, (b) infrared.

(a)

(b)

(a)

(b)

Figure 17. SMS-GOES images of NSSL analysis area at 2330 GMT with (a) visible, (b) infrared (heightened grey level intensities).

that the cloud cover was variable enough to allow for the generation of simulated radiances and the subsequent retrievals even as the supercell moved across the grid.

The temperature field (850 mb as seen in Figures 18 and 19) depicts a warm area (297°K — 24°C) advecting to the east, while slightly cooler air (21°C) drifted in over the grid in association with the storm system. Warm air then swept back over the domain from the west, related to the downburst outflow of the supercell and the motion of the dryline. The dewpoint temperature field (850 mb as seen in Figures 20 and 21) underwent dramatic changes as dry air (T_D = 0°C) moved off to the east, while moist air (T_D = 18–20°C) pushed in behind the dry air and ahead of the storm system. A tongue of dry air then flowed back into the western sections by 2330 GMT.

The vertical cross-sections of the mixing ratio (Figures 22 and 23) provide a clear depiction of the low level convergence and resultant increase in moisture, which are apparent from a well-defined bulge of mixing ratio values rising to 18g/kg. These extreme values may indicate a tendency of the objective analysis scheme to over-inflate interpolated calculations in areas of large gradients or high concentrations. The tilting with height of the moisture bulge was only slightly noticeable in the present case. Over the 3-hour period, the moist bulge advected across the region in association with the subsident outflow of the supercell and the intrusion of the dryline. The thin layer of moist air that remained positioned over the surface even after the passage of the moist bulge was most likely a result of the precipitation being generated over the area.

The equivalent potential temperature (θ_e) fields (Figure 24) readily present the influence of the supercell as it proceeded across the network. An interesting feature was the slight rise in values of θ_e at the low levels before a bulge of the largest readings followed across. As in the previous example, mixing by the severe convective storm was apparent, especially by 0100 GMT May 30, 1976 when the western half of the grid became a fairly homogeneous field in θ_e. Excessive values of
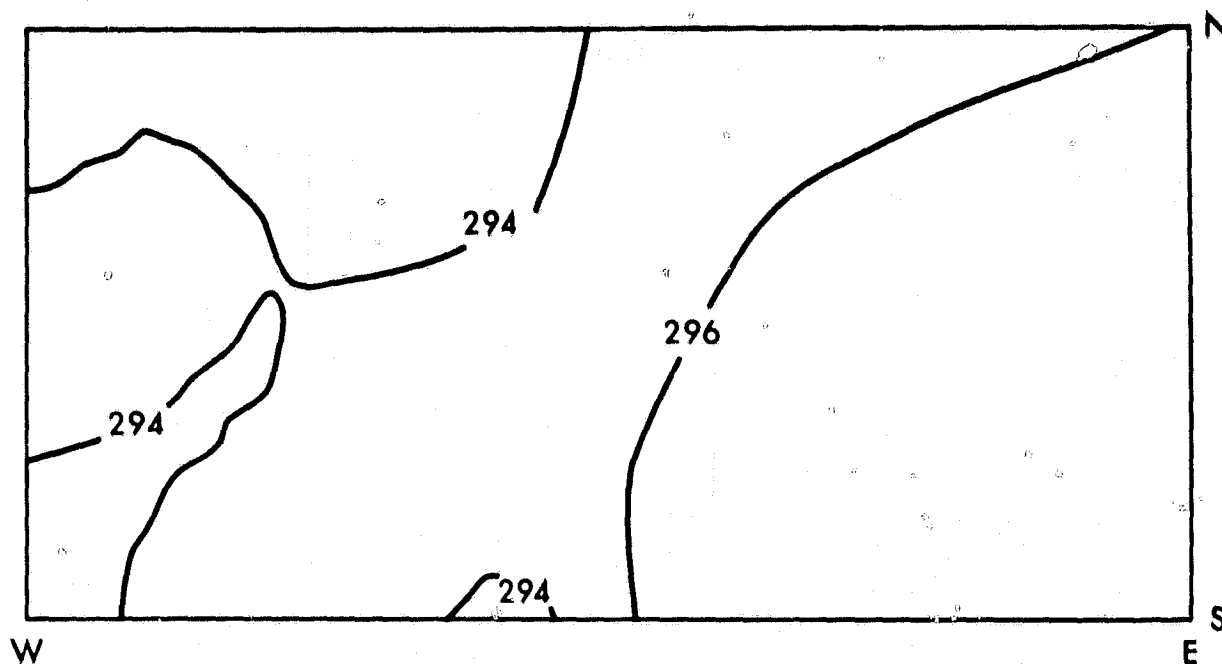
23

Figure 18. 850-mb temperature (K) analysis for special NSSL grid at 2030 GMT 29 May 1976.
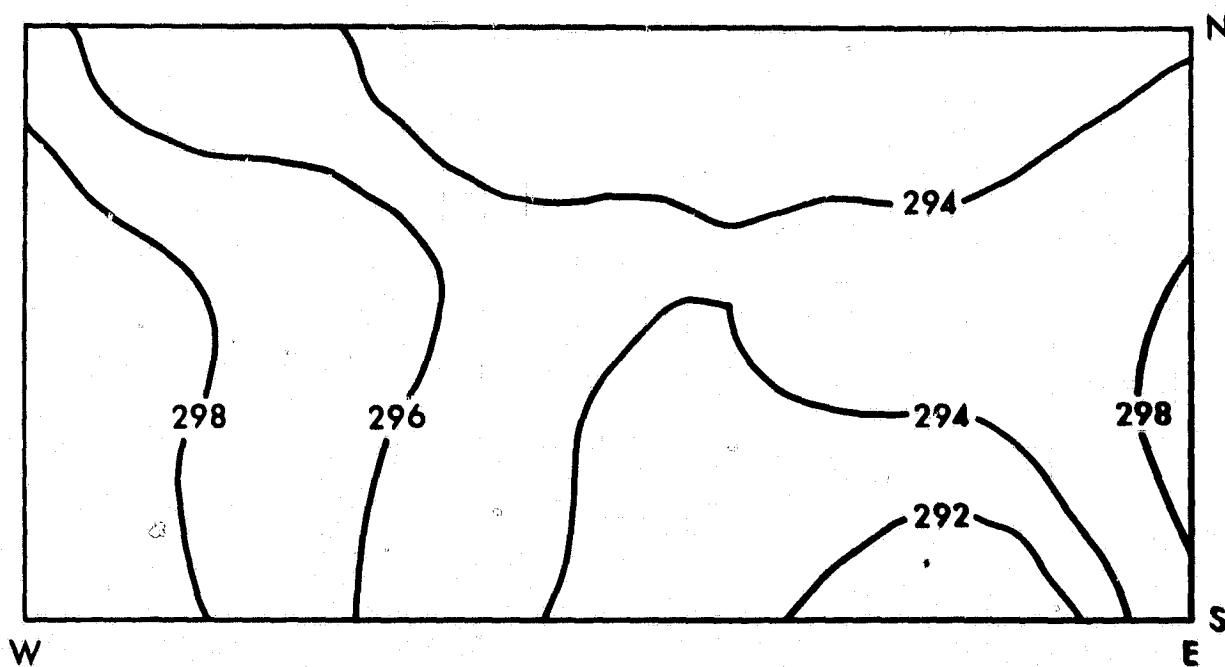

Figure 19. 850-mb temperature (K) analysis for special NSSL grid at 2330 GMT.
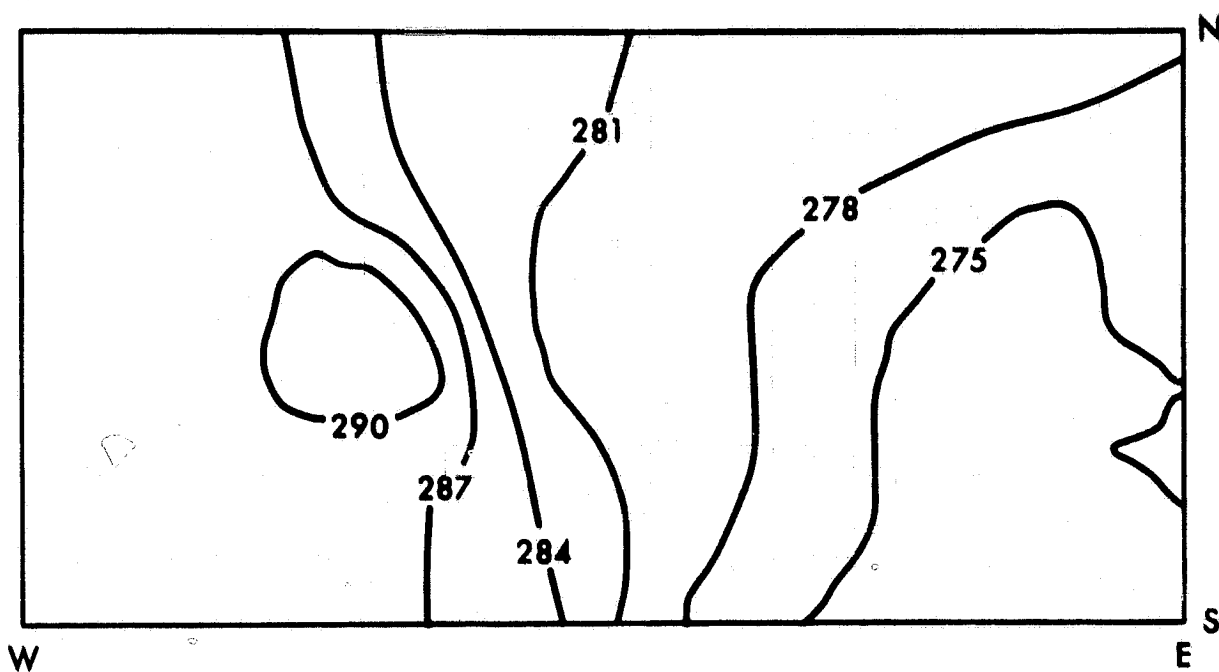
Figure 20. 850-mb dewpoint temperature (K) analysis for special NSSL grid at 2030 GMT 29 May 1976.
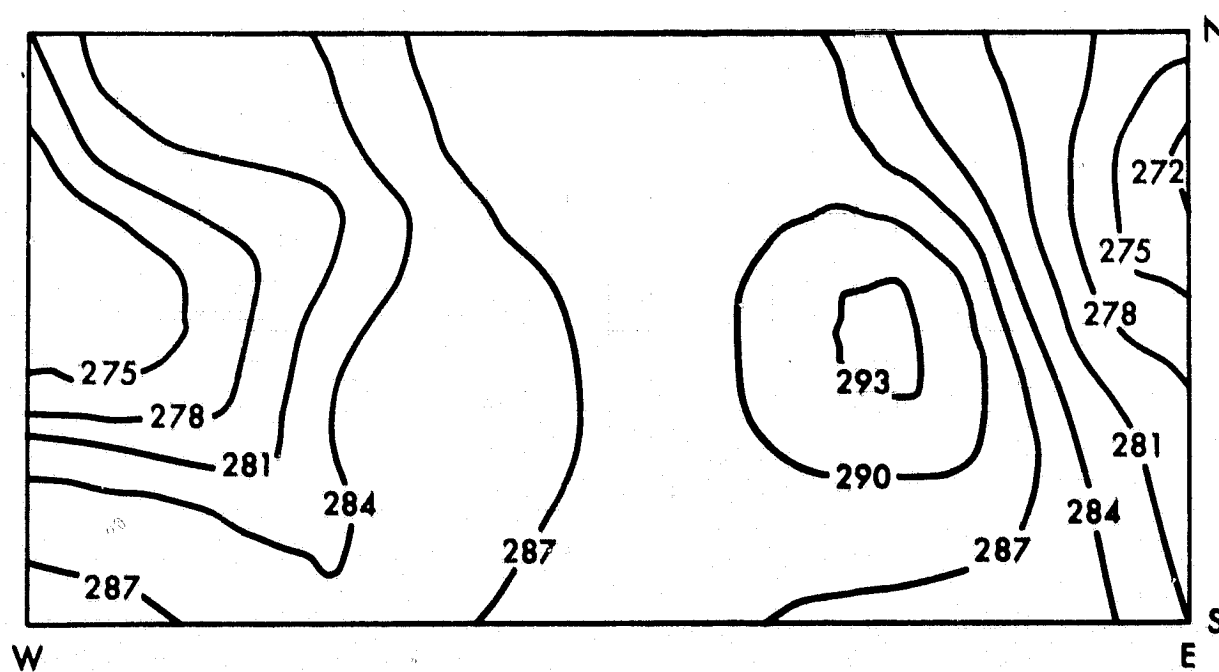

Figure 21. 850-mb dewpoint temperature (K) analysis for special NSSL grid at 2330 GMT.
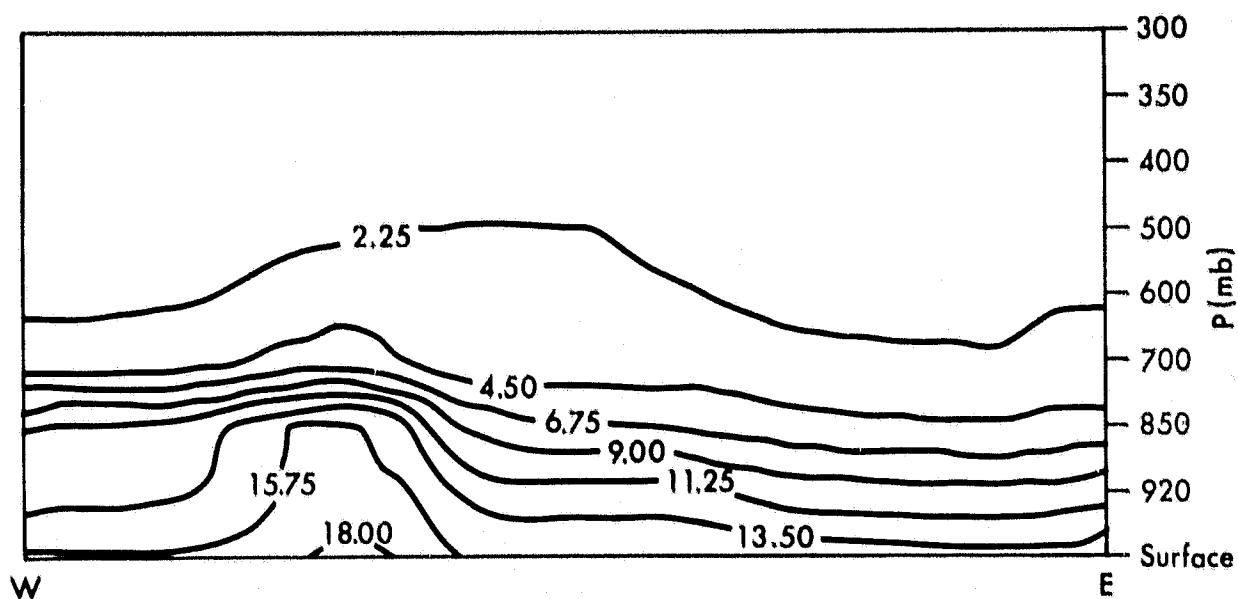
Figure 22. Vertical west-east cross-section of mixing ratio field (g/kg) through the center of the special NSSL grid at 2030 GMT 29 May 1976.

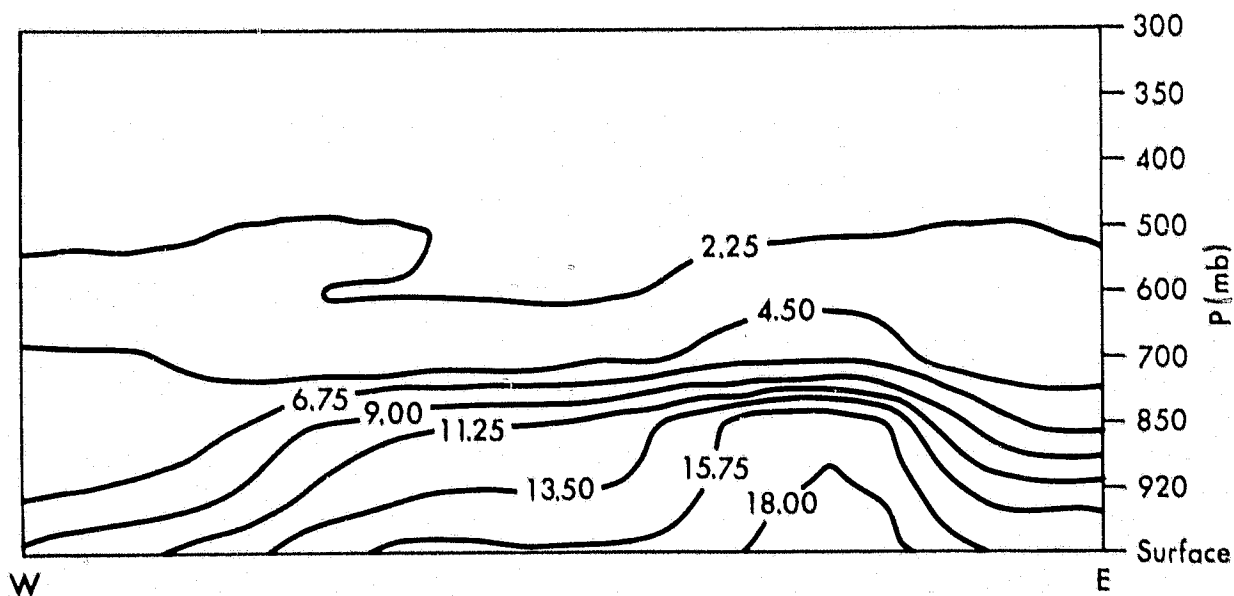Figure 23. Vertical west-east cross-section of mixing ratio field (g/kg) through the center of the special NSSL grid at 2330 GMT.
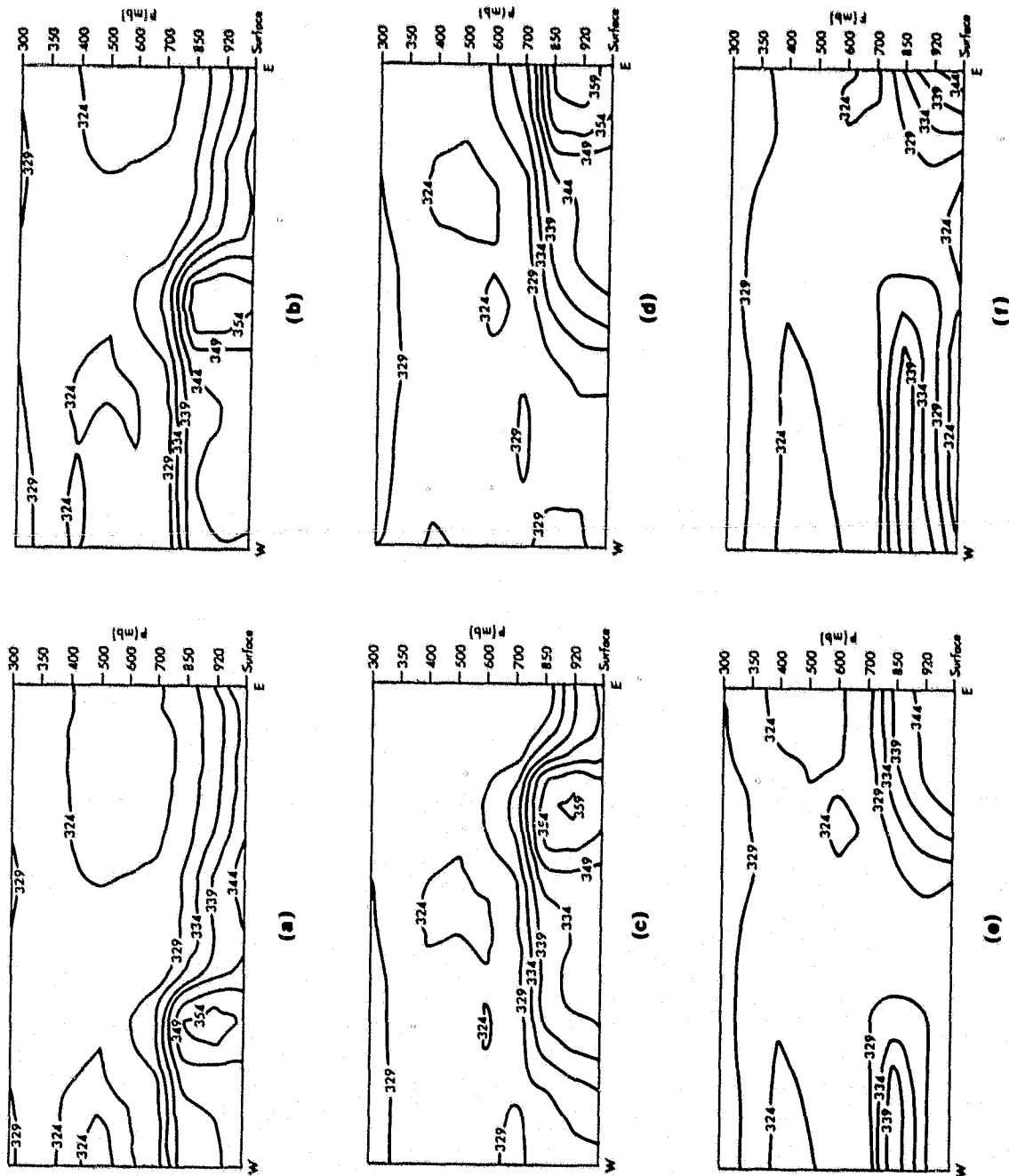
Figure 24. Vertical west–east cross-sections of equivalent potential temperature (K) field through the center of the special NSSL grid at the following times: (a) 2030 GMT 29 May 1976, (b) 2200 GMT, (c) 2330 GMT, (d) 0100 GMT 30 May 1976, (e) 0230 GMT, (f) 0400 GMT.

27

θ_e at 2330 GMT (May 29) and 0100 (May 30) with values of θ_e as great as 359°K (86°C) resulted because of the correspondingly large mixing ratios observed in Figures 22 and 23.

An important difference between the two cases selected for this investigation is that the analyzed time slots for the second (May 29*th*) case are 180 minutes apart instead of the 90 minutes of the previous date. This longer time step produced enhanced fluctuations in the meteorological fields. Sharp temperature and moisture gradients were more apparent in the later case and, combined with the satisfactory cloud-cover conditions, provide an excellent example of a severe storm atmosphere for the simulated VAS retrieval study.

5. SUMMARY

In this technical memorandum, eight cases of severe convective storms that occurred over the 1976 NSSL network are documented in preparation for a simulated VAS retrieval study (Chesters *et al.*, 1980). Since the retrieval of temperature and moisture profiles from radiance data using regression techniques is non-unique, ancillary data must be utilized to constrain the solution. The statistical nature of meteorological sounding sets can be incorporated directly into the retrieval technique through the derivation of linear regression matrices based solely upon soundings that are representative of specific meterological events such as severe storms. The data sets from the NSSL network provide mesoscale temperature and moisture fields, which are representative of the severe storm environment, and can be incorporated into retrieval schemes to possibly yield more accurate temperature and moisture soundings within the resolution expected from VAS.

Six of the cases provide meteorological data for a control set that will produce the statistical information needed for the regression retrievals. Two independent "target" dates (May 22 and 29, 1976) were selected for the simulation experiment on the basis of moisture gradients over the NSSL

network and the availability of satellite images that provide the cloud–cover information needed for the simulation experiments. Two time slots on May 29, 1976 appear to present the optimum conditions for the retrieval investigation. The cloud cover at these times is not too extensive, while sharp moisture gradients exist over the NSSL analysis region. The data sets thus provide a severe storm environment that will test the sensitivity of the VAS regression retrieval technique to the different regression matrices, the results of which are presented by Chesters *et al.*, (1980).

ACKNOWLEDGMENT

REFERENCES

1. Alberty, R., J. Weaver, O. Sirmans, J. Wooley, and B. Bumorner, *Spring Program 1976*, National Oceanic and Atmospheric Administration, Technical Memorandum ERL NSSL–83, 1977.

2. Barnes, S. L., J. H. Henderson, and R. J. Ketchum, *Rawinsonde Observation and Processing Techniques at the National Severe Storms Laboratory*, National Oceanic and Atmospheric Administration, Technical Memorandum ERL NSSL–53 (NTIS COM–71–00707), 1971.

3. _____, *Mesoscale Objective Map Analysis Using Weighted Time–Series Observations*, National Oceanic and Atmospheric Administration, Technical Memorandum ERL NSSL–62, 1973.

4. Chesters, D., and S. Carter, *Radiance Simulation on the VAS Processor*, National Aeronautics and Space Administration, Technical Memorandum (Manuscript in preparation).

5. _____, A. Mostek, and L. Uccellini, *Simulated Mesoscale Gradient Retrievals on the VAS Processor*, National Aeronautics and Space Administration, Technical Memorandum (Manuscript in preparation).

6. _____, and W. Robinson, *Cloud Correction Algorithms for VAS*, National Aeronautics and Space Administration, Technical Memorandum (Manuscript in preparation).

7. Computer Sciences Corporation, CSC/TM-79/6095, *Mesoscale Case Studies, Interim Report 3*, W. P. Gross, 1979.

8. Lee, Tay-How, and D. Chesters, *Comparison of Regression and Conditioned Least-Squares Retrievals on the VAS Processor*, National Aeronautics and Space Administration, Technical Memorandum (Manuscript in preparation).

9. Ogura, Y. and M. Liou, "The Structure of a Midlatitude Squall Line: A Case Study," *Monthly Weather Review;* March 1980, (pp. 553-567).